Accepted Manuscript

The effect of light sensitizer localization on the stability of indocyanine green liposomes

Tatu Lajunen, Riikka Nurmi, Danny Wilbie, Teemu Ruoslahti, Niklas G. Johansson, Ossi Korhonen, Tomasz Rog, Alex Bunker, Marika Ruponen, Arto Urtti

The effect of light sensitizer localization on the stability of indocyanine green liposomes

Tatu Lajunen[a], Riikka Nurmi[a], Danny Wilbie[b], Teemu Ruoslahti[a], Niklas G. Johansson[c], Ossi Korhonen[d], Tomasz Rog[ef], Alex Bunker[a], Marika Ruponen[d], Arto Urtti[adg]

[a]Division of Pharmaceutical Biosciences, Drug Research Program, Faculty of Pharmacy, University of Helsinki, Helsinki, Finland
[b]School of Pharmacy, Utrecht University, Utrecht, Netherlands
[c]Division of Pharmaceutical Chemistry and Technology, Drug Research Program, Faculty of Pharmacy, University of Helsinki, Helsinki, Finland
[d]School of Pharmacy, University of Eastern Finland, Kuopio, Finland
[e]Department of Physics, Tampere University of Technology, Tampere, Finland
[f]Department of Physics, University of Helsinki, Helsinki, Finland
[g]Biomedical Chemistry Laboratory, Institute of Chemistry, St. Petersburg State University, St. Petersburg, Russia

Abstract

Light triggered drug delivery systems offer attractive possibilities for sophisticated therapy, providing both temporal and spatial control of drug release. We have developed light triggered liposomes with clinically approved indocyanine green (ICG) as the light sensitizing compound. Amphiphilic ICG can be localized in different compartments of the liposomes, but the effect of its presence, on both triggered release and long term stability, has not been studied. In this work, we report that ICG localization has a significant effect on the properties of the liposomes. Polyethylene glycol (PEG) coating of the liposomes leads to binding and stabilization of the ICG molecules on the surface of the lipid bilayer. This formulation showed both good storage stability in buffer solution (at +4-37 °C) and adequate stability in serum and vitreous (at +37 °C). The combination of ICG within the lipid bilayer and PEG coating lead to poor stability at elevated temperatures of +22 °C and +37 °C. The mechanisms of the increased instability due to ICG insertion in the lipid bilayer was elucidated with molecular dynamics simulations. Significant PEG insertion into the bilayer was induced in the presence of ICG in the lipid bilayer. Finally, feasibility of freeze-drying as a long term storage method for the ICG liposomes was demonstrated. Overall, this is the first detailed study on the interactions of lipid bilayer, light sensitizer (ICG) and PEG coating on the liposome stability. The localization of the light triggering agent significantly alters the structure of the liposomes and it is important to consider these aspects in triggered drug delivery system design.

1. Introduction

Targeted delivery of drugs using external light trigger is feasible in light-accessible organs, *e.g.* eye and skin, and it may offer several benefits compared to passive drug leakage from the drug carrier. In principle, laser triggered drug release might enable therapy adjustments according to the progression of the disease and cyclic changes in the body [1]. The parameters of the laser based remote triggering (*i.e.* beam diameter, exposure duration, wavelength and light intensity) can be adjusted in a versatile manner for the specific drug delivery system and target tissue [2-4].

Liposomes are a robust and well-studied class of drug delivery systems (DDS) [5-7]. They are used in many drug therapies, including the treatment of cancer, infections and other diseases [8-10]. Liposomes can be prepared using a variety of methods and the resulting formulation properties can be adjusted with processing parameters [11]. Passive drug release from liposomes is often erratic and inadequate [6,12], but the release can be enhanced by using external triggering mechanisms [13]. Various light triggering mechanisms for liposomes have been developed, *i.e.* photo-cleavage, polymerization and energy conversion to heat [5,14-19]. In particular, infrared (IR) light has been found to be a very attractive triggering method, due to superior tissue penetration and safety [5,20].

We have previously developed light triggered liposomes using indocyanine green (ICG) as the light sensitizing agent for delivery and fast release of small compounds and macromolecules [21,22]. The formulation released small and macromolecular contents after five seconds of near infra-red light exposure [22]. ICG is a fluorescent dye that has been approved by European Medicines Agency (EMA) and the U.S. Food and Drug Administration (FDA) for clinical imaging [23,24] related to angiography and lymphatic function [25-28]. This indicates that ICG is safe to use in humans. The use of ICG in light activated liposomes is based on the ability of ICG to convert absorbed light energy (at about 800 nm) to heat [27-32]. Due to its amphiphilic structure, ICG can be integrated into the liposomal lipid bilayer or be wrapped into the polymeric coating of the liposomes, for example polyethylene glycol [22] that is used to increase the circulation time of intravenously administrated liposomes in the blood stream [33,34]. Obviously, the light triggered liposomes should release their contents based on light triggering, but otherwise they should show adequate chemical, physical and physiological stability [35]. ICG degrades upon light activation [21], but the effect of ICG on the liposome stability has not been elucidated previously.

We investigated the impact of ICG on the stability of the liposomes in the presence of buffers, serum and vitreous humour of the eye. Different sites of ICG localization in the liposomes (lipid bilayer or polymeric sheath) were investigated experimentally and *in silico* using molecular dynamics simulations. Furthermore, freeze drying of the liposomes was explored as potential stabilization procedure.

2. Materials and methods

2.1. Materials

1,2-Dipalmitoyl-sn-glycero-3-phosphocholine (DPPC), 1,2-distearoyl-sn-glycero-3-phosphocholine (DSPC), 1-stearoyl-2-hydroxy-sn-glycero-3-phosphocholine (lyso-PC), 1,2-distearoyl-sn-glycero-3-

phosphoethanolamine (DSPE) and 1,2-distearoyl-sn-glycero-3-phosphoethanolamine-N-[methoxy(polyethylene glycol)-2000] (DSPE-PEG) were bought from Avanti Polar Lipids, Inc. (Alabaster, AL, USA). All other compounds were bought from Sigma-Aldrich (St. Louis, MO, USA).

2.2. Preparation of ICG liposomes

The lipids were dissolved in chloroform in molar ratios of 75:15:10:4 (DPPC / DSPC / Lyso PC / DSPE-PEG or DSPE) prior to the liposome preparation. The liposomes were formed by the thin film hydration method followed by extrusion through a polycarbonate membrane as described earlier [22]. ICG was integrated into the lipid bilayers using the following procedure. ICG (0.2 µmol) was dissolved in methanol and mixed with the lipids in chloroform prior to evaporation of the organic solvent. For ICG entrapment to the PEG layer, the same amount of ICG was added to the aqueous hydration solution. The thin lipid layer was hydrated with 500 µL of HEPES buffer solution (20 mM HEPES, 140 mM NaCl, pH 7.4) or calcein solution (60 mM, 280 mOsm/kg, pH 7.4). The lipids and hydration solution were incubated in a +60 °C water bath forming polydisperse liposomes. The liposomes were extruded 11 times at +60 °C through a polycarbonate membrane with pores of 100 nm (diameter) with a syringe-type extrusion device (Avanti Polar Lipids). Thereafter, the liposomes were quickly cooled and stored in a refrigerator. The free calcein and ICG in the liposome suspension were removed by gel filtration through a Sephadex G-50 (Sigma-Aldrich) column, where HEPES buffer solution was used for elution. The lipid concentration of the purified samples was 1.5 mM, and the ICG concentration was 30 µM.

2.3. Analysis Methods

2.3.1. Temperature-Induced Content Release

Contents release from the liposomes was studied at temperatures ranging from +35 to +50 °C on a thermomixer with an Eppendorf heating block (Eppendorf AG, Hamburg, Germany) as described earlier [22]. Briefly, the calcein encapsulating liposomes were heated for 10 minutes while shaking at 300 rpm. Following this their fluorescence was measured with a Varioskan Flash plate reader (Thermo Fisher Scientific Inc., Waltham, MA, USA), and the release percentage (R) was calculated as

$$R = \frac{F_t - F_0}{F_{100} - F_0} \times 100\% \quad (1)$$

where F_t is the fluorescence of the sample at a specific measurement time point, F_0 is the background fluorescence of the sample, and F_{100} is the fluorescence of complete release of the model drug compound by disruption of the lipid bilayer with 10 µL of 10% Triton-X.

2.3.2. Light-Induced Content Release

The light-induced contents release was determined as described earlier [5]. Briefly, the purified liposome sample (500 µL) was placed in the thermomixer (Eppendorf AG) and heated to +37 °C. The light-triggering was done with 808 nm light for 5 s using a laser power of 9.7 W/cm^2 (Modulight, Tampere, Finland). The fluorescence of released calcein was analyzed with a Varioskan Flash plate reader and release patterns were calculated with Equation 1.

2.3.3. Differential Scanning Calorimetry

Differential scanning calorimetry (Mettler Toledo DSC823e, Mettler-Toledo GmbH, Greifensee, Switzerland) was used to determine the phase transition temperatures (T_m) of the liposomes. Briefly, 20 µL of the liposome sample was pipetted to aluminum pan and sealed by an aluminum lid with two small holes to prevent pressure buildup. The sample and reference pans were heated using a linear temperature gradient alongside a reference pan in a nitrogen environment. The phase transitions were seen as endothermic peaks in the thermographs (analyzed with STARe software, Mettler Toledo). The phase transitions of the freeze-dried samples were analyzed from powder samples after reconstitution with purified water.

2.3.4. Size Analysis and Zeta Potential of Liposomes

The size of the liposomes for the stability studies was analyzed with a Zetasizer APS dynamic light scattering automated plate sampler (Malvern Instruments, Malvern, United Kingdom) and reported as size distributions by particle number and polydispersity index (PdI). The zeta potential was measured with Zetasizer ZS (Malvern Instruments). The size and the zeta potential of the liposomes before and after freeze-drying process were measured with a Zetasizer Nano ZS (Malvern Instruments), because these experiments were carried out at a different location.

2.3.5. Stability of ICG

The ICG degrades quickly in aqueous solutions and loses its absorbance peak at 800 nm [36]. Absorbance is used to measure the leakage from the liposomes and degradation of the ICG molecules. The ICG amount was analyzed using a Varioskan Flash plate reader in black clear bottom well plates (Corning Inc., Corning, NY, USA). Absorbance of 100 µL samples were measured at a wavelength of 800 nm. The amount of remaining ICG compared to the initial concentration (ICG_R) was calculated as

$$ICG_R = \frac{ICG_t}{ICG_0} \times 100\% \qquad (Equation\ 2)$$

where ICG_t is the absorbance at the specific time point and ICG_0 is the absorbance at the start of the experiment.

2.4. Stability of Liposomes in Buffer Solution, Vitreous and Serum

The liposomes with ICG and encapsulated calcein (25% of the total volume, 0.375 mM) were incubated up to 15 days in HEPES buffer, porcine vitreous or human serum at +4, +22, and +37 °C. Samples were collected and analyzed at several time points during the storage. The size distribution of the liposomes, calcein release (Equation 1), and ICG stability (Equation 2) were determined during the storage as described above.

2.4.1. Isolation of the Porcine Vitreous

The porcine vitreous was obtained using a method described earlier with modifications [37]. Fresh porcine eyes were bought from a slaughter house (HK Ruokatalo, Forssa, Finland) and refrigerated during the transport. Extraocular tissue was cleaned from the eyes with scissors, and the eyes were dipped in ethanol and then in phosphate buffered saline (PBS) before cutting the eye ball. The eyes

were cut circumferentially behind the limbus, and then the anterior part of the eye and the lens were removed. The vitreous was removed from the eye cup and pooled into a plastic tube. The pooled vitreous humor was homogenized with a glass plunger on an ice bath. The vitreous was centrifuged at 3200 x g (+4 °C) for 60 min. The resulting supernatant was filtered through 0.45 µm and 0.22 µm syringe filters and stored at -80 °C before use. The pH of the vitreous is known to change from neutral pH to about 8 after removal from the eye [38]. The studied liposomes and ICG are not pH sensitive [36], and thus this change in pH is unlikely to significantly affect the results.

2.4.2. Human Serum

Blood was drawn from seven healthy and fasted male human donors using Vacutainer glass tubes without clot activator (BD, Franklin Lakes, NJ, USA). Permission for research use of blood was obtained from Helsinki University Hospital. The volunteer donors had provided their informed consent for research use and the samples were anonymized. The blood was left to clot for 30 min at +22 °C. The blood samples were first centrifuged at $2500 \times g$ for 5 min and the supernatant was collected. The supernatant was centrifuged again at $3500 \times g$ for 5 min. Collected serum fractions from all donors were pooled under aseptic conditions and stored in aliquots at -80 °C.

2.5. Degraded ICG exposure

Intense light exposure at about 800 nm has been shown to degrade the ICG molecules [21]. Therefore, the effect of degraded ICG molecules on content leakage from the liposomes was determined. In order to generate degraded ICG, the molecules in HEPES buffer without the liposomes were exposed to laser light (808 nm, 9.7 W/cm^2) for 20 min. Calcein containing ICG liposome formulations with and without PEG were incubated for 1h or 24h at +37 °C with 15 µM, 30 µM, 60 µM or 300 µM of initial ICG. The calcein release was measured and calculated as described above.

2.6. Molecular Dynamics Simulation of the ICG and Lipid Bilayer

To provide added insight into the effect of ICG localization and PEG on the liposome bilayer we performed additional analysis of the MD trajectories described in our previous study [22]. In brief, the simulated system consisted of a lipid bilayer composed of 22 DSPE-PEG, 78 DSPC, 52 lyso PC, and 360 DPPC molecules, hydrated by 52447 water molecules with a physiological salt concentration; 8 ICG molecule were present in the system and 172 Na$^+$ and 142 Cl$^-$ ions were added to achieve both the desired salt concentration and charge neutrality. Two models of a PEGylated bilayer were constructed. In the first ICG was placed in the water phase (Formulation A), and in the second ICG was placed inside the lipid bilayer (Formulation C). As a reference system, we a used a bilayer with the same composition, but without PEGylation (Formulation B): all DSPE-PEG lipids were replaced by DSPC. All molecules and ions were parameterized using the all-atom optimized potentials for liquid simulations (OPLS-AA) force field [39] with additional parameters derived specifically for lipids [40,41]. The TIP3P model of water was used [42]. All simulations were performed using the GROMACS 4.6.6 software package [43]. Once equilibration was achieved, all systems were simulated for a total of 100 ns at a temperature of +37 °C and 1 bar pressure. Further details regarding ICG parameterization, system setup, and all other simulation protocols not mentioned here are provided in the previous study [22].

In order to characterize the properties of the lipid bilayers, we used several analysis tools available within the GROMACS 4.6.6 suite; these include measuring the mass density profile and molecular order parameter. Additionally, we visualized the system using VMD 1.9.3. The molecular order parameter, S_{CD}, is defined as

$$S_{CD} = \langle \frac{3}{2}(cos^2\theta_i) - \frac{1}{2} \rangle \qquad (Equation\ 3)$$

where θ_i is the angle between a C-D bond (C-H in simulations) of the ith carbon atom and the bilayer normal. The angular brackets denote averaging over time and over relevant C-D bonds in the bilayer. The mass density profile is a measure of the number of a specific atom, atom group, or entire molecules located at specific positions normal to the plane of the lipid membrane, *i.e.* where the molecule sits in the membrane.

2.7. Freeze-drying of ICG liposomes

Empty liposomes, which were diluted with Milli-Q water after extrusion, were freeze-dried in a Linkam thermal stage (THMS350 V, Linkam Scientific Ltd., Tadworth, Surrey, UK), which was connected to a liquid nitrogen pump, temperature controller and vacuum pump. The settings were controllable through the Linksys software provided by Linkam. A 15 mm diameter object glass was used as base for the sample and placed directly on the heating block. Two freezing ramps to -40 °C were tested: 10 °C/min and 2 °C/min. Drying was done at -20 °C and 0 °C for the primary and secondary drying steps respectively. Duplicates were freeze-dried for each combination of lyoprotectant concentration, lyoprotectant type (sucrose and trehalose, Sigma-Aldrich) and freezing rate. Trehalose and sucrose were chosen as lyoprotectans since they are widely used in the literature [44-46]. Lyoprotectant stock solutions (0.9 M) were added to the liposome solutions at molar ratios of 1:3, 1:5, 1:7, 1:10 and 1:20, corresponding to sucrose or trehalose concentrations of 4.5, 7.5, 10.5, 15 and 30 mM, respectively.

2.8. ^{31}P NMR spectroscopy

^{31}P NMR spectroscopy was used to characterize the phospholipid bilayer of the liposomes [47-50]. Concentrated samples of the formulations without calcein were prepared in 700 μL of D_2O as described above (60 μmol of total lipids). The ^{31}P NMR spectra were acquired on a Bruker Ascend 400 MHz – Avance III HD NMR spectrometer (Bruker Corporation, Billerica, MA, USA) at 161.98 MHz equipped with a 5 mm BBO SmartProbe™ with z-axis gradients. A zgpg30 pulse sequence including broadband ^{31}P–^{1}H decoupling was used for the acquisition. The FID files were acquired with acquisition parameters set to 2048 scans, 5 s relaxation delay and measured at +27, +37, +39 and +50 °C, respectively. The recorded FID files were processed with MestReNova 12.0.1 software (Mestrelab Research, Santiago de Compostela, Spain) to obtain the reported spectra.

2.9. Statistical Analyses

In the freeze-drying experiments the results were analyzed using GraphPad Prism 5. To assess the effect of sugar concentration on particle size and PdI, one-way ANOVA with Tukey post-hoc testing was applied. To assess the difference between the two sugars or freezing rates at different concentrations, two-way ANOVA with Bonferroni post-hoc testing was used. The post-hoc tests were

only done when the ANOVA was significant. In the other experiments Student's *t* test was used to evaluate the statistical significance between the sample groups. The differences between the results were considered to be significant when the p-values were less than 0.05.

3. Results

3.1. Characterization of the ICG liposomes with variable ICG localizations

Three formulations with different ICG loading methods were prepared (Table 1). Formulation A consisted of PEGylated liposomes with ICG in the aqueous hydration solution, which means that the ICG is bound and stabilized by the PEG chains outside the lipid bilayer [22]. Liposomes in formulation B were lacking PEG, and ICG was mixed with the phospholipids prior to the chloroform evaporation. In formulation C, the ICG was mixed with the phospholipids and the liposomal composition included also PEG. The formulations had comparable amounts of ICG with measured absorbance (800 nm) of 0.31 ± 0.05, 0.31 ± 0.02 and 0.28 ± 0.03, for formulations A, B and C, respectively. The liposomes had homogenous initial sizes of about 100 nm with the formulation B showing the largest mean diameter (Table 1). All formulations had a slightly negative surface charge in the range of -3.28 mV to -4.68 mV (Table 1).

Table 1. Inclusion of PEG, the loading method of the ICG, size and the zeta potential of the prepared formulations.

Formulation	PEG included	ICG in aq. solution	ICG mixed with the lipids	Diameter (nm), PdI	Zeta potential (mV)
A	X	X		**96 ± 26**, 0.047 ± 0.006	-4.44 ± 2.23
B			X	**123 ± 32**, 0.083 ± 0.029	-4.68 ± 0.34
C	X		X	**103 ± 26**, 0.101 ± 0.044	-3.28 ± 0.54

^{31}P NMR spectra of the phosphate group motion in the bilayers of all formulations was measured (Supplementary material, Figure S1). Formulations A and C showed a sharp peak at about -1 ppm at all measured temperatures. Formulations B and C showed a broad signal at -10 ppm at temperatures +27, +37 and +39 °C, while formulation A only at +27 °C. All formulations had a tall peak at -1 ppm without broad signal at temperature of +50 °C.
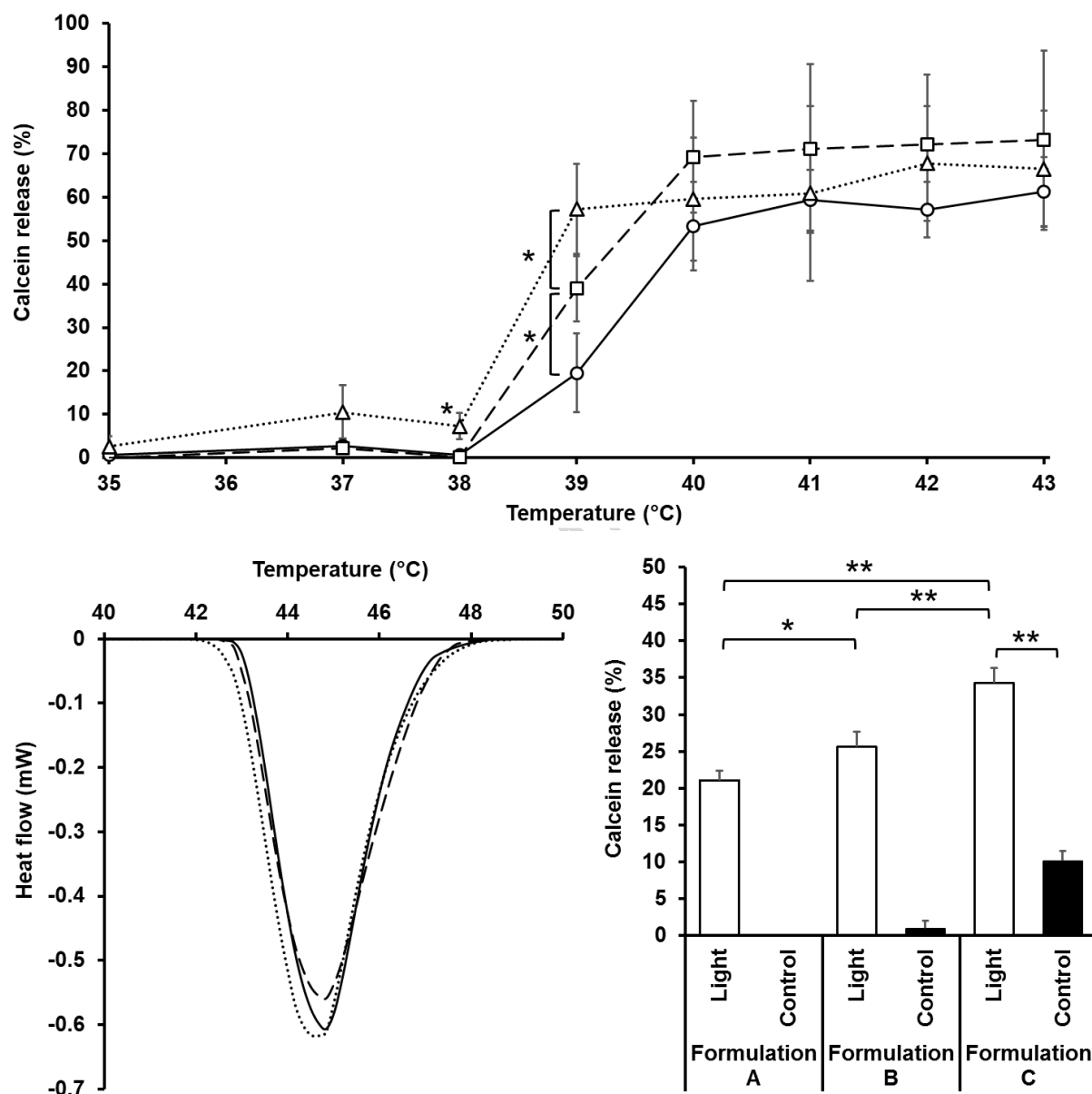

Figure 1. **Top:** Calcein release in various temperatures of formulation A (circle, solid line), formulation B (square, dashed line) and formulation C (triangle, dotted line). The error bars represent the standard deviations (n = 3, *p < 0.05). **Bottom left:** Differential scanning calorimetry measurements of the liposome formulations. Heat flow graphs of formulation A (solid line), B (dashed line), and C (dotted line) (n=3). **Bottom right:** Light-triggered calcein release from the formulations. The control samples

were shielded from the light and kept at the same temperature (+37 °C) during the light exposure. The error bars represent the standard deviations (n = 3, *p < 0.05 and **p < 0.005).

Calcein release from the liposomes at increasing temperatures was measured (Figure 1, top). Formulations A and B showed good stability up to +37 °C, and calcein release was increased at higher temperatures. Formulation C was the leakiest one, showing 10% release at +37 °C and 57% at the temperature of +39 °C. Formulations A and B at +39 °C released 20% and 39% of the calcein, respectively.

The differential scanning calorimetry measurements showed only negligible differences between the formulations (Figure 1, bottom left). The onset of the phase transition started at +42-43 °C for all formulations. Likewise, the peaks of phase transitions were at same temperature for all formulations.

After light exposure (5 s of 808 nm laser light at +37 °C) calcein release from the liposomes was 21%, 26% and 34%, for formulations A, B and C, respectively (Figure 1, bottom right). Notably, formulation C showed significant passive calcein release of about 10% during the experiment.

3.2. Stability of liposomes in various matrices

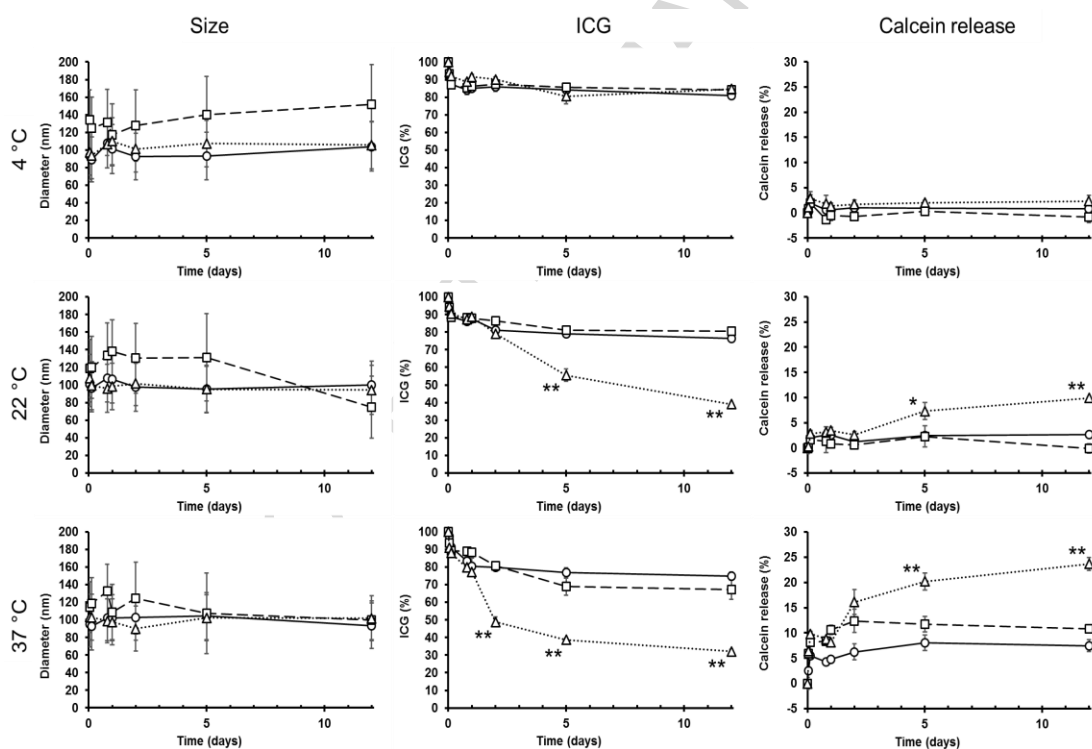### 3.2.1. Stability in aqueous buffer solution

Figure 2. Stability of formulations A (circle, solid line), B (square, dashed line), and C (triangle, dotted line) during 12 days in HEPES buffer (20 mM HEPES, 140 mM NaCl, pH 7.4) at +4 °C (top row), +22 °C (middle row), and +37 °C (bottom row). Mean size of the liposomes (left), the stability of ICG (center), and the contents release (right) were measured. The error bars represent the standard deviations (n = 3, *p < 0.05 and **p < 0.01).

The stability of all formulations was studied for 12 days at +4, +22 and +37 °C (Figure 2). Each formulation retained their initial size (Table 1) during the test. The absorbance of ICG for 800 nm light disappears upon its degradation [21] allowing stability measurements. Degradation of about 10% was seen during the first day in all formulations at all temperatures (Figure 2). At +4 °C, the ICG remained stable from 1 day onwards, whereas after 12 days at +22 and +37 °C significant ICG degradation was seen in formulation C (40% and 32% of ICG remaining at +22 and +37 °C, respectively) and slower degradation in formulations A and B.

No significant calcein release was observed during 12 days at +4 °C (Figure 2). At +22 °C, formulations A and B remained stable, but formulation C leaked 10% of the calcein dose during 12 days. At +37 °C, all of the formulations showed some contents leakage. After 12 days formulations A, B and C, had leaked 7%, 11% and 24% of the calcein, respectively.

3.2.2. Stability in porcine vitreous and human serum

The stability of all formulations was studied in two relevant biological environments, serum and vitreous, at +37 °C (Figure 3). No significant change in size was seen in 6 days, but the liposomes seem to become more polydisperse (average PdI of 0.47). This may be due to the interference of serum and vitreal components, and thus the actual size of the liposomes may not be reliably assessed. After 6 days, the samples showed increasing amount of cloudiness and sedimentation from presumed natural aggregates of the serum and the vitreous, thus preventing further size analyses.
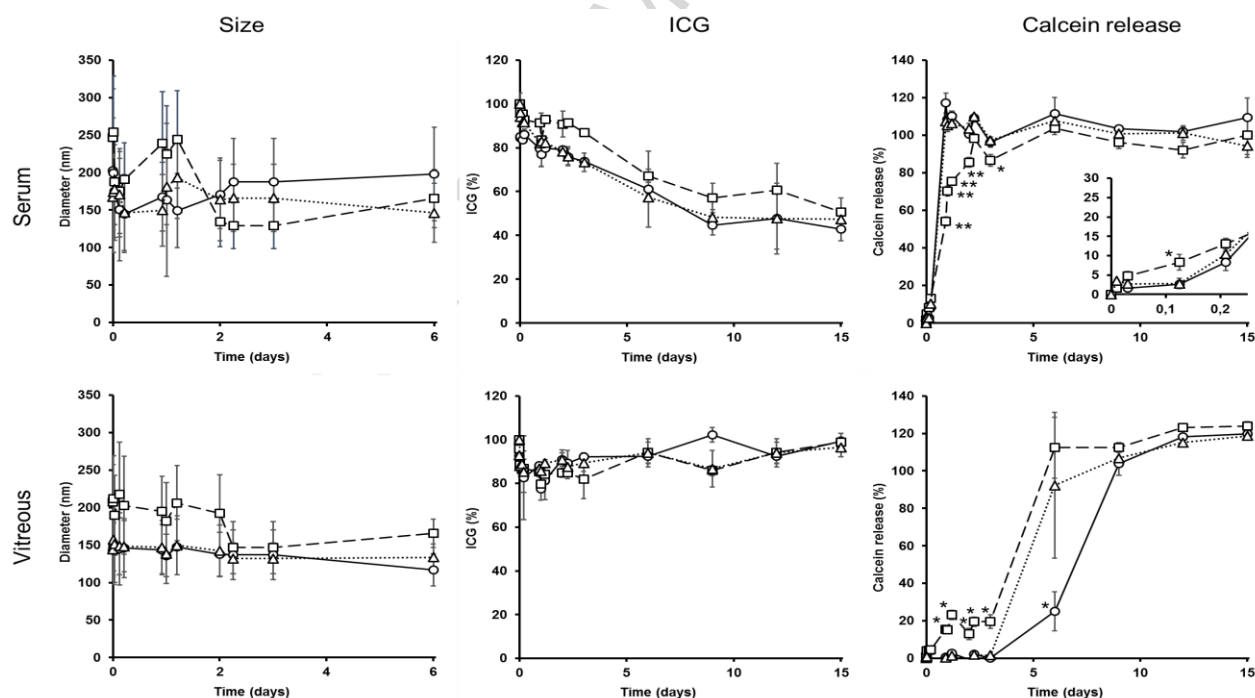

Figure 3. Stability of formulations A (circle, solid line), B (square, dashed line), and C (triangle, dotted line) at +37 °C in serum (top row) and vitreous (bottom row). Mean size of the liposomes (left), the stability of ICG (center), and the contents release (right) were measured. The error bars represent the

standard deviations (n = 3, *p < 0.05 and **p < 0.01). The insert in the top rightmost graph shows the calcein release during the first 5 hours.

The amount of intact ICG decreased by 50-60% in serum during 15 days in all formulations. The stability of the liposomal ICG was better in the vitreous, as more than 90% of ICG remained intact in all formulations for 15 days. All formulations behaved in a similar manner in terms of ICG stability.

Calcein release from the liposomes was studied in serum and vitreous. The formulations were relatively stable in serum for 5 hours, but thereafter significant release was observed already during the first day (Figure 3). Again, stability of the liposomes was better in the vitreous: formulations A and C did not show any calcein leakage up to 3 days whereas formulation B leaked 20% of the calcein dose in three days. At 6 days, all calcein had released from formulations B and C, while only 25% leaked from formulation A. At day 9, all calcein had leaked out also from formulation A.

3.3. Molecular dynamics (MD) simulations

Results of the computational MD modelling are shown in figure 4. The results for the calculation of the mass density profiles (Figures 4A and 4C) show peaks within the membrane in addition to outside the membrane for the PEG distribution. This indicates that some of the PEG polymers have entered into the lipid core of the membrane. This phenomenon has been observed in PEGylated membrane systems that we have studied in our previous computational work [43,51,52]. Visualizations of the lipid membrane (Figures 4B and 4D) show this phenomenon as well. Additionally, the visualization shows that the membrane does not remain in the fluid phase but has the structure of a gel or ripple phase. In our prior studies of bilayers in the gel phase we did not observe the PEG polymer penetration into the bilayer on the timescale over which the simulations were performed [51,53], however, the initial setup of these studies was different: these systems were initiated in the gel phase with the PEG lipids oriented outwards, into the water. In the current study, the model was initialized at an elevated temperature and gradually cooled down; in this respect, a better model of the relevant experimental method of thin film hydration and extrusion. PEG penetration into the highly ordered, but not gel phase, bilayer with cholesterol present, however, has been observed in our prior studies [52].
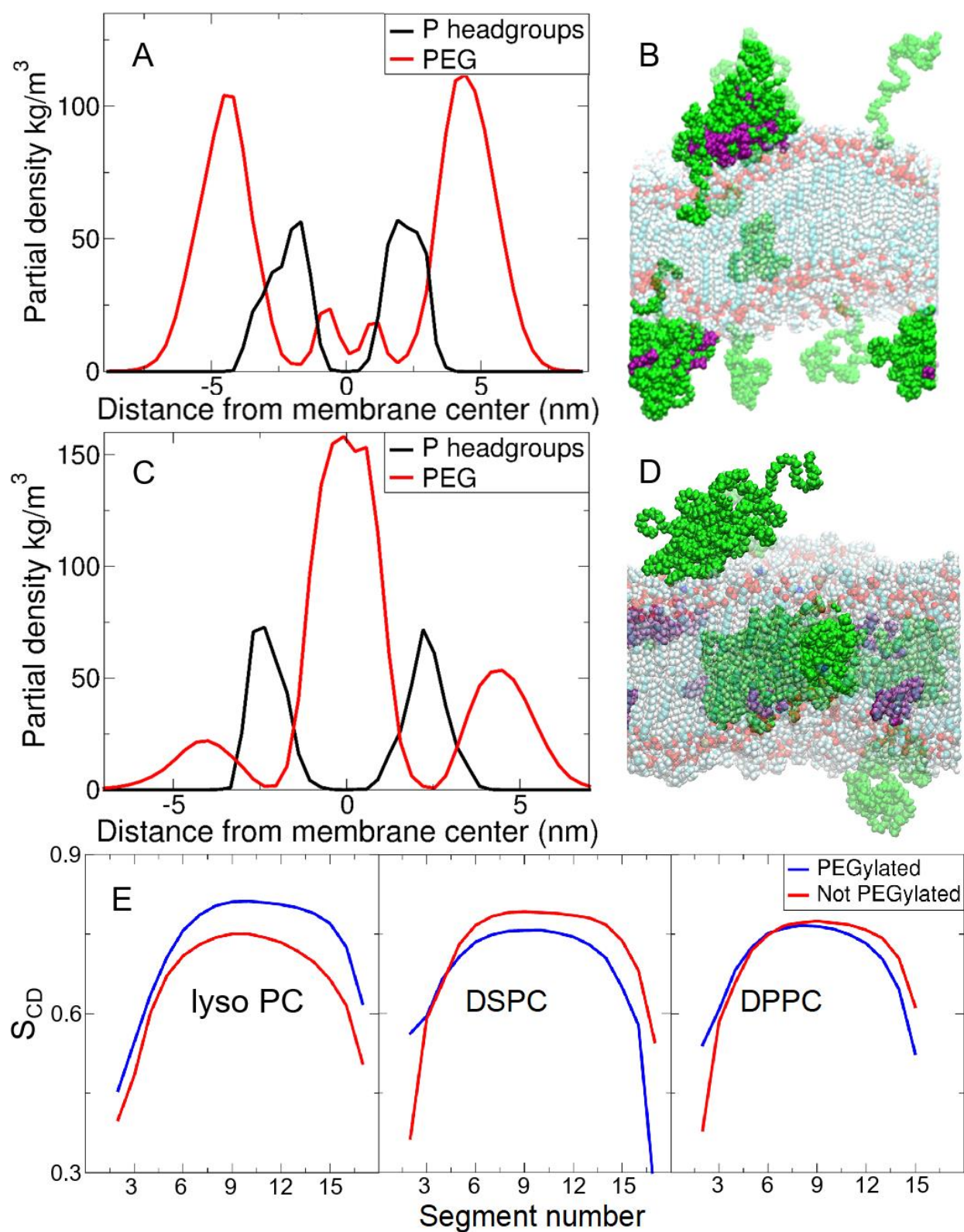
Figure 4. Mass density profile for the PEGylated membrane with ICG in the water phase (A), and visualization of the PEGylated membrane (B). PEG polymers are shown in green, ICG shown in purple and phosphate head groups in red. Mass density profile and membrane visualization for PEGylated

membrane with ICG inside the lipid bilayer (C and D). Molecular order parameter for the three systems constituent lipids of the membrane with ICG inside the lipid bilayer (E).

Results for the molecular order parameter (Figure 4E), indicate that PEGylation affects this parameter for all non-PEG lipid constituents in the membrane (lyso PC, DSPC, DPPC). The molecular order parameters are noticeably increased for lyso PC and decreased for DSPC when PEG is included in the formulation.

3.4. Effect of degraded ICG on contents leakage

Our experiments showed that ICG degradation and the fastest contents leakage took place in formulation C (Figure 2). Therefore, the effect of ICG degradation products on the release of calcein was determined. Liposomes with the same phospholipid compositions with and without PEG were incubated with degraded ICG at different concentrations.
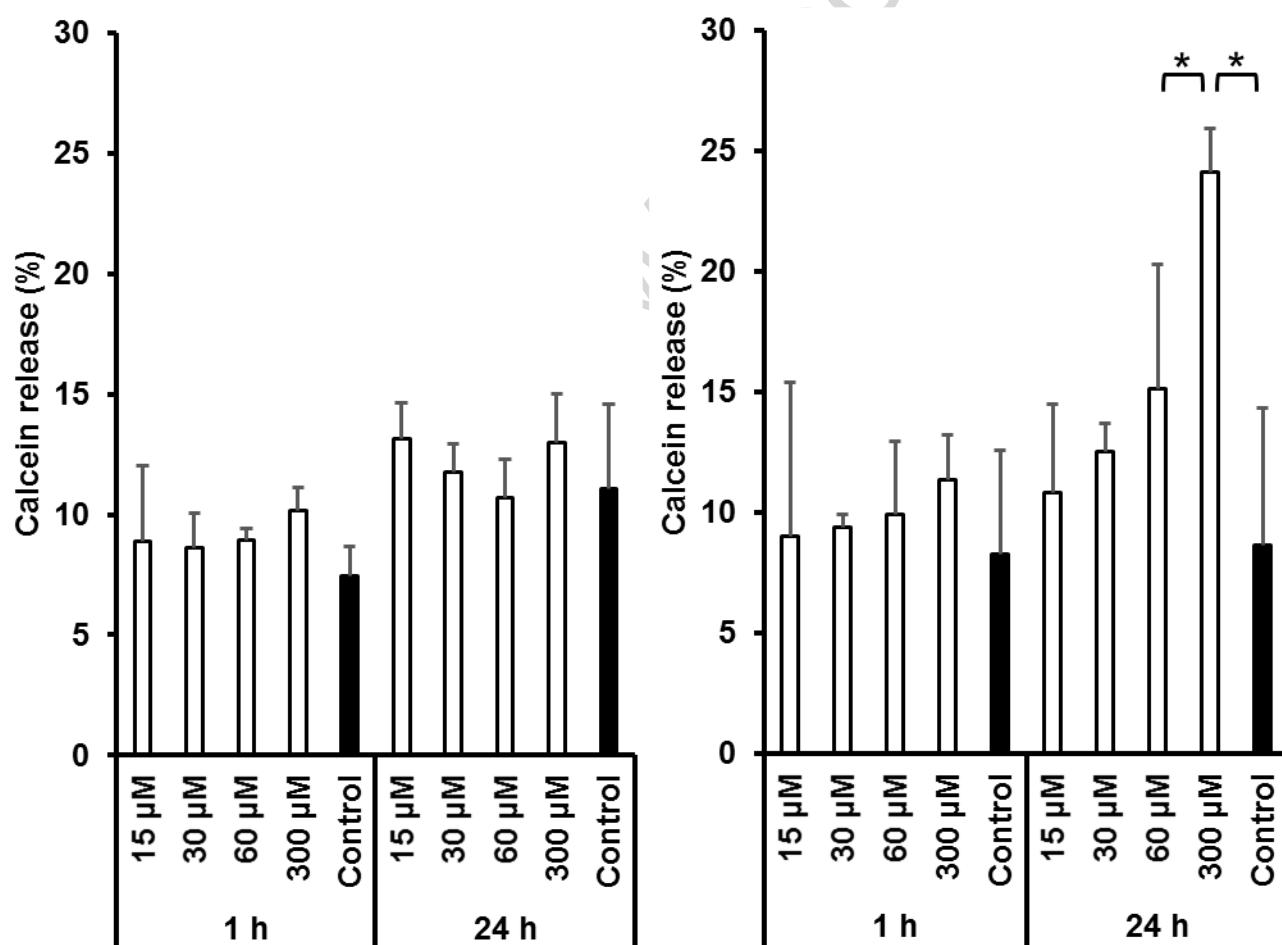

Figure 5. The effect of degraded ICG on the contents leakage from the formulations with PEG (left) and without PEG (right) during 1 h and 24 h in +37 °C. The amount of initial ICG is shown under the horizontal axis. Control samples were without any degraded ICG. The error bars represent the standard deviations (n=3, *p < 0.01).

PEGylated liposomes released calcein at the levels of about 10-13 % during 24 hours (Figure 5). Degraded ICG did not increase calcein release. In the case of the liposomes without PEG, presence of ICG degradation products caused increasing trend in calcein leakage during 24 h in concentration dependent manner (Figure 5). The difference was significant at 300 µM of ICG degradation products. Thus, only high concentrations of degraded ICG increase calcein leakage in the liposomes without PEG.

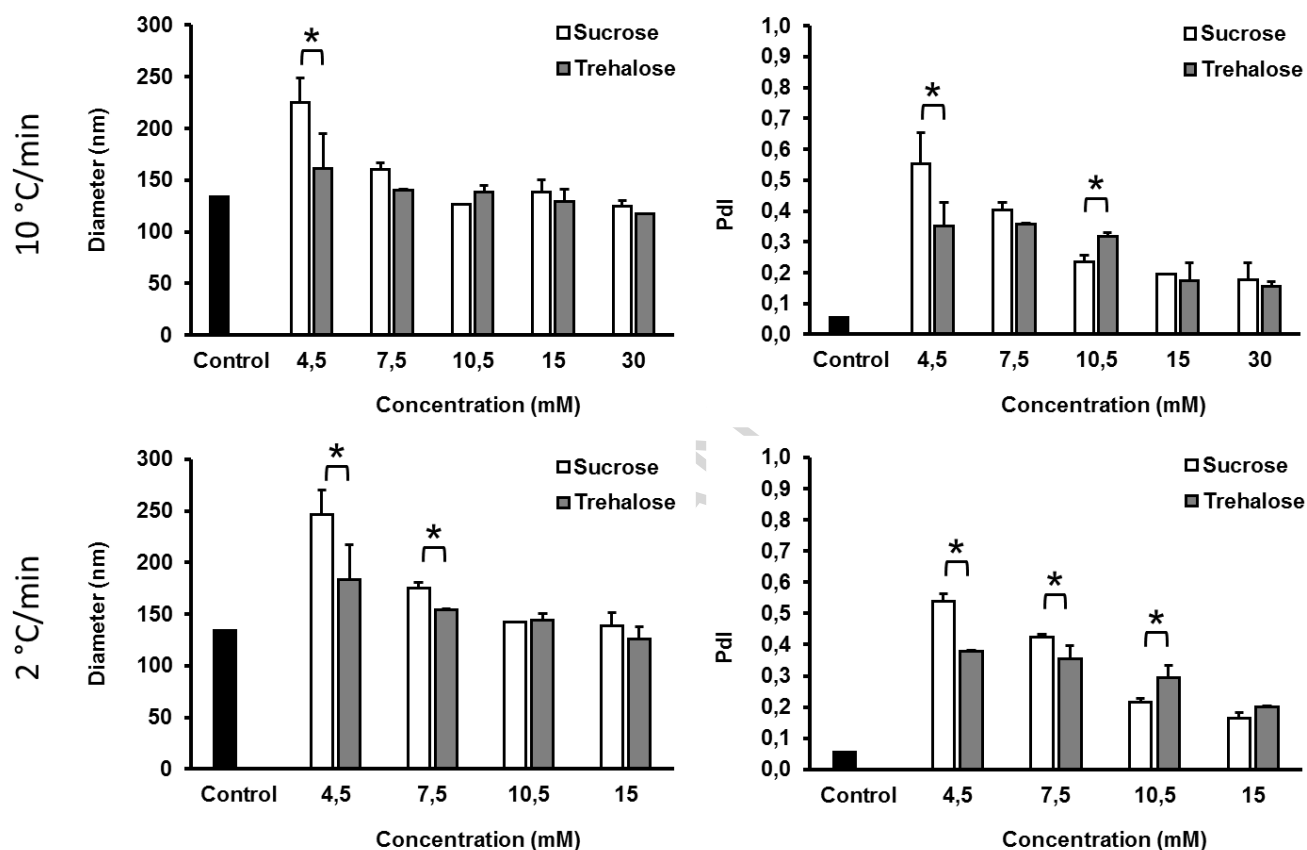### 3.5. Freeze-drying of ICG liposomes

Figure 6. The particle diameter and PdI of liposomes freeze-dried at the rate of 10 °C/min (top) and 2 °C/min (bottom). The control samples were not freeze-dried. The error bars represent the standard deviations (n=2, *p < 0.05).

Freeze-drying is considered to be an effective method to improve the shelf-life stability of liposomes [54]. The most promising formulation A was selected for freeze drying experiments. Freeze-drying was performed using trehalose and sucrose as lyoprotectants, but without encapsulated calcein. The average onset temperatures for phase transitions (+42.9-43.9 °C) did not show differences between the groups (control, sucrose, trehalose).

The mean particle diameter and PdI were determined for each lyoprotectant formulation at two freezing rates (Figure 6). Freeze-drying without any lyoprotectants increased the mean particle size 10-fold and the PdI was 1.0. At a freezing rate of 10 °C/min, the particle size of sucrose samples ranged between a 1.8-fold increase (4.5 mM) to no change compared to the control (10.5 mM and 30 mM) (Figure 6, top). The general trend shows that the low sucrose concentrations leads to larger particles after freeze-drying.

Increasing the lyoprotectant concentration above 10.5 mM does not yield much added benefit. The trehalose samples showed a similar trend at all concentrations, with the exception of 4.5 mM, where they show only a 1.2-fold increased size in comparison to the control sample. The PdI of all freeze-dried samples was higher than the control samples, ranging an 8-fold increase (4.5 mM) to a 2-fold increase (15 mM and 30 mM). The zeta potential of the liposomes remained unchanged after the freeze-drying (data not shown).

Similar trends can be seen for the samples with the slower freezing rates of 2 °C/min (Figure 6, bottom). The size of liposomes in the presence of 15 mM of sucrose or trehalose was slightly increased (1.1-fold) compared to the control, while significant increase was seen with the lyoprotectant concentration of 4.5 mM. The PdI showed the same trend as the other freezing rate. Retention of hydrophilic calcein was shown to be poor during the freeze-drying process (Supplementary material) with most the cargo escaping upon reconstitution of the dry powder.

4. Discussion

Drug delivery to the posterior segment of the eye is challenging, but on the other hand the transparent eye is very well suited for the use of light triggered DDS [55]. Likewise, cancer is a unique target for drug delivery, which often requires very potent drug substances with possible severe adverse effects. Site-specific drug release could help in reducing drug doses and adverse drug effects. Treatment of various skin conditions is applicable for external light induced drug release. Furthermore, light triggered liposomes can be applied during surgery with fiber optics and the drug could be released at the desired place and time. If suitable stability properties of the DDS can be achieved while retaining the necessary sensitivity for the light activation, ICG liposomes may offer an attractive solution to several drug delivery problems. It has been known for a long time that inclusion of PEG coating or cholesterol in the bilayer improve the liposomal stability in biological environments [56-59]. Unfortunately, cholesterol hinders the heat based release method during light activation. An optimal balance must be found with the stability and light triggering sensitivity. In this study, the localization of the ICG molecules has shown to have an impact on the stability of the liposomes, even though the formulations retain their light activated release functions regardless of the localization of the ICG.

In this paper, three different formulations of ICG encapsulation method were studied. Previous results have shown that the ICG in the aqueous solution is wrapped by the PEG chains (Formulation A) showing only limited interaction with the lipid bilayers [22]. If a PEG corona is not present, the ICG will be embedded within the bilayer (Formulation B). If ICG is mixed with the phospholipids in the presence of PEGylated lipids (Formulation C), the localization ICG is difficult to determine. The molecular dynamics simulations suggest that the ICG remains in the bilayer, at least for short time periods. Significant ICG migration may occur between the lipid bilayer and the PEG corona over long time periods. The differences in the results between formulations A and C indicate that not all ICG molecules escape from the lipid layers to the PEG corona in formulation C. The zeta potentials of the liposomes were in the same range. The slightly higher mean diameter of the formulation B could be attributed to the lack of steric stabilization and some liposome aggregation, but the size differences

were not significant. ICG or ICG derivatives can be covalently conjugated with phospholipids [60-63]. In theory, these formulations would have similar effects on the phospholipid bilayer as formulation A, but they are outside the scope of this article. The ICG – lipid conjugates are planned to be characterized in the follow up studies.

Phospholipids in liposomal bilayers show ^{31}P chemical shift anisotropy patterns due to their orientation in the magnetic field of NMR [49,50,64]. In liposomal phospholipids the spectra usually exhibit sharp peaks and broad signals depending on the phospholipid molecule types and the interactions with the surroundings and size of the liposome. All of the formulations had a phosphate peak at 0 ppm due to the rapid tumbling of liposomes with about 100 nm diameter [65] (Figure S1). The tall peaks at lower ppm found in spectra of formulation A and C are due to the DSPE-PEG structure [64,66,67]. The broad signal at about -10 ppm indicates restricted movement of the phospholipids and amine phosphate interactions between phospholipids or with other molecules [47,64,68,69]. At increased temperatures the phospholipids move more freely in the bilayer resulting in a reduction of the broad signal with formulation A. In case of formulations B and C, the broad signal at elevated temperatures (+37 and +39 °C) may be due to interaction between the phosphate of the lipids and the amine of ICG [68,69]. Thus, it is uncertain if phospholipid movement is increased or not in those cases. In case of formulation C, the broad signal in the ^{31}P NMR spectra shows that ICG is located at the lipid bilayer instead of the PEG corona (Figure S1-C).

The localization of ICG had an effect on the leakage of calcein from the liposomes during a heat gradient experiment (Figure 1). Formulation A and formulation C were the most and the least stable, respectively. Notably, formulation C released some calcein already at +37 °C suggesting that premature contents release could take place *in vivo*. The DSC results showed T_m lowering of only a 1 °C for formulation C as compared to formulations A and B. The actual difference in the lipid bilayer fluidity may be more significant, since DSC is not sensitive enough to detect the ripple phase that is normally present below T_m [15]. Even though differences were seen in the light activation experiments (Figure 1), all formulations had acceptable light triggering properties. Formulation C was the most sensitive formulation in terms of light triggered release, but it also had the most prominent passive leakage at +37 °C. This result is in accordance with the heat release and calorimetric experiments.

Similarly, the storage in aqueous buffer at temperatures +4, +22 and +37 °C showed inferior stability of formulation C (Figure 2). Degradation of ICG and the leakage of calcein were most pronounced with formulation C at +22 and +37 °C. The size of the formulations remained unchanged, which indicates that the leakage from formulation C is mediated by the bilayer changes and not due to the aggregation processes. Because the difference between formulations B and C is the presence of the PEG, the increased ICG degradation in formulation C is due to the effect of the PEG molecules. Furthermore, the difference between formulations A and C is the location of the ICG molecules. Thus, it can be speculated that some level of PEG interaction with the bilayer is enabled by the lipid embedded ICG molecules. This interaction may cause leakage of ICG molecules into the aqueous solution and eventual degradation [36]. The slightly larger diameter of formulation B may be due to the lack of steric stabilization by PEG coating, leading to some aggregation of the liposomes.

In serum and vitreous, larger liposomal diameters of about 150-200 nm were observed. This may be due to adherence of biological compounds [70,71]. In the vitreous, the ICG remained stable, while all

of the formulations showed decrease in ICG absorbance in the serum. About half of the ICG was degraded at 15 days in the vitreous. Furthermore, calcein retention was poor in the serum and much better in the vitreous: most calcein leaked out in one day in the serum, whereas complete release took 6-9 days in the vitreous. The serum has higher protein concentration (60-80 g/L) than the vitreous (0.28-1.36 g/L) [55,72-76]. The proteins may adhere to the liposomes [71], interact with the bilayers and induce leakage [77,78]. Formulation B showed higher initial contents leakage, in both serum and vitreous, compared to formulations A and C. Formulation B lacks the PEG coating making it more sensitive to attachment of serum and vitreous components. In vitreous, the PEG formulations were very stable for 3 days, which would be a reasonable time frame for liposomes to reach the retinal targets after intravitreal injections [55]. The formulations were relatively stable up to 5 hours in serum, which may be enough for the liposomes to reach the common target sites [8,79]; the temporal margin for the light activation is clearly shorter in the blood circulation than in the vitreous.

Overall, the passive calcein leakage was the most prominent from formulation C with PEG corona and ICG in the bilayer (Table 1). The passive leakage would be undesirable in therapy, as it would lead to uncontrolled drug release off-target. Molecular dynamics simulations were used to elucidate the possible reasons for these phenomena (Figure 4). PEG remains, for the most part, outside the phospholipid bilayer in case of formulation A and do not disrupt the ordered lipid layer and cause passive leakage (Figures 4A and 4B). In the case of formulation C, when ICG is within the PEGylated lipid bilayer (Figures 4C and 4D), significant PEG penetration into the bilayer was also seen. The ICG is localized near to the liposomal surface, theory of which is supported by ^{31}P NMR data indicating ICG interaction with the phospholipid head groups. Because all the components of the bilayer affect the stability of the liposome [12,80], ICG may cause a slight disruption in the ordered phospholipid phase, thereby enabling insertion of PEG into the lipid layer and its further disruption. In the visualization image from molecular dynamics simulations, large areas of the bilayer have the PEG molecules displacing the phospholipids (Figure 4D). As PEG is significantly more hydrophilic than the phospholipids, these PEG domains may allow the leakage of hydrophilic calcein from the liposomes. Likewise, the PEG insertion into the bilayer may pull out some ICG and increase the degradation rate of the ICG (Figure 2). However, it seems that the degraded ICG did not induce the leakage of calcein (Figure 5) and it is unlikely that the degraded ICG has any major consequences on liposome stability.

Altogether we see, from the computational modelling results, evidence that PEG disrupts the membrane structure, possibly affecting the phase behavior of the bilayer. This could manifest itself as a decrease of the temperature of the main phase transition (Figure 1), a broadening of the temperature range of the transition or a decrease in the latent heat associated with the transition. This provides evidence that PEGylation of the membrane will, in fact, increase the extent to which the membrane structure would potentially be disrupted by presence of the ICG in the membrane. This in turn leads to less stability during the storage at elevated temperatures (Figures 2 and 3). The phenomena was also shown in our previous studies [22], where although the ICG was placed in the water phase, passive contents leakage was seen with very high ICG concentrations. Obviously, there is a limit on the binding capacity of the PEG and any unbound ICG localizes to the lipid bilayer causing instability.

The molecular order parameter was changed due to the inclusion of PEG into the bilayer (Figure 4E). For the case of a lipid bilayer in the gel phase, a change characterized by a collective tilt of the acyl tails that adopt an all-*trans* conformation was seen. This indicates a disruption of the gel structure, but

detailed interpretation of the observed collective tilt and evaluation of its significance in relation to the liposomal stability is difficult. The hydrophilic PEG domains within the bilayer are the more likely route of calcein leakage than the altered conformation of the acyl tails. Nevertheless, the results show that the PEG insertion affects the phospholipid ordering and this change may be significant for other bilayer properties [81].

We also assessed freeze-drying of formulation (A) as means of stabilization. Sucrose and trehalose were selected as lyoprotectants, since these have been used in intravitreal anti-VEGF injections (Eylea, Lucentis and Avastin). The impact of the freezing rate was studied, because it may affect the conservation of lipid bilayers [54,82]. In our study, no difference between the freezing rates was seen in terms of liposomal size, polydispersity and T_m (Figure 6). Overall, the freeze-drying did not affect the T_m of the liposomes, which is in accordance with previous results [54,83]. The particle size of the liposomes was preserved by adding at least 15 mM of sucrose or trehalose, although the PdI was slightly increased (Figure 7). 15 mM was about the equivalent of a 2:9 lipid-lyoprotectant ratio (w/w), based on their molecular weights and concentrations. The ratio is on the lower side of the findings in the literature that have reported ratios ranging from 1:5 to 1:10 [83,84]. Even though the size of the liposomes remained unchanged, significant calcein leakage was noted during the freeze-drying process (Supplementary material). Calcein crystallizes as water is removed and is poorly reconstituted leading to low retention. Although, the calcein retention during the freeze-drying was poor, the process is probably suitable for ICG liposomes encapsulating lipophilic drugs. Those preferably remain in the lipid bilayer and the temporary disruption of the ordered state does not cause content leakage.

5. Conclusions

The stability of ICG liposomes with different ICG molecule loading protocols was studied. The most stable formulation included PEG coating and ICG inclusion in the hydration solution. The stability in common storage conditions (+4 °C and +22 °C) was acceptable. In biological environments, vitreous and serum at +37 °C, the liposomes remained sufficiently stable for 3 days and 5 hours, respectively. This should be adequate for the most common clinical treatment protocols. The content leakage mechanisms were elucidated with *in vitro* and *in silico* experiments, and PEG penetration into the lipid bilayer was found to be possible major cause for the instability. The interaction of PEG and lipid membrane localized molecules should be taken in to account during formulation design. Finally, freeze-drying was determined to be applicable for long term storage of ICG liposomes, although further research is needed to determine viable cargoes.

Supplementary material

^{31}P NMR spectroscopy results and the protocol and results of freeze-dryed calcein loaded liposomes are shown in the supplementary material.

References

[1] S. Mura, J. Nicolas, P. Couvreur, Stimuli-responsive nanocarriers for drug delivery, Nature materials. 12 (2013) 991-1003.

[2] C. Alvarez-Lorenzo, L. Bromberg, A. Concheiro, Light-sensitive intelligent drug delivery systems, Photochem. Photobiol. 85 (2009) 848-860.

[3] P. Shum, J. Kim, D.H. Thompson, Phototriggering of liposomal drug delivery systems, Adv. Drug Deliv. Rev. 53 (2001) 273-284.

[4] T. Spratt, B. Bondurant, D.F. O'Brien, Rapid release of liposomal contents upon photoinitiated destabilization with UV exposure, Biochimica et Biophysica Acta (BBA)-Biomembranes. 1611 (2003) 35-43.

[5] T. Lajunen, R. Nurmi, L. Kontturi, L. Viitala, M. Yliperttula, L. Murtomäki, A. Urtti, Light activated liposomes: functionality and prospects in ocular drug delivery, J. Controlled Release. 244 (2016) 157-166.

[6] A. Samad, Y. Sultana, M. Aqil, Liposomal drug delivery systems: an update review, Current drug delivery. 4 (2007) 297-305.

[7] A. Bunker, A. Magarkar, T. Viitala, Rational design of liposomal drug delivery systems, a review: combined experimental and computational studies of lipid membranes, liposomes and their PEGylation, Biochimica et Biophysica Acta (BBA)-Biomembranes. 1858 (2016) 2334-2352.

[8] H.I. Chang, M.K. Yeh, Clinical development of liposome-based drugs: formulation, characterization, and therapeutic efficacy, Int. J. Nanomedicine. 7 (2012) 49-60.

[9] S.K. Soininen, K. Vellonen, A.T. Heikkinen, S. Auriola, V. Ranta, A. Urtti, M. Ruponen, Intracellular PK/PD relationships of free and liposomal doxorubicin: quantitative analyses and PK/PD modeling, Molecular pharmaceutics. 13 (2016) 1358-1365.

[10] G. Bozzuto, A. Molinari, Liposomes as nanomedical devices, Int. J. Nanomedicine. 10 (2015) 975-999.

[11] T. Lajunen, K. Hisazumi, T. Kanazawa, H. Okada, Y. Seta, M. Yliperttula, A. Urtti, Y. Takashima, Topical drug delivery to retinal pigment epithelium with microfluidizer produced small liposomes, European Journal of Pharmaceutical Sciences. 62 (2014) 23-32.

[12] V.P. Torchilin, Recent advances with liposomes as pharmaceutical carriers, Nature reviews Drug discovery. 4 (2005) 145-160.

[13] A. Gomez-Hens, J. Fernandez-Romero, Analytical methods for the control of liposomal delivery systems, TrAC Trends in Analytical Chemistry. 25 (2006) 167-178.

[14] L. Paasonen, T. Laaksonen, C. Johans, M. Yliperttula, K. Kontturi, A. Urtti, Gold nanoparticles enable selective light-induced contents release from liposomes, J. Controlled Release. 122 (2007) 86-93.

[15] L. Paasonen, T. Sipilä, A. Subrizi, P. Laurinmäki, S.J. Butcher, M. Rappolt, A. Yaghmur, A. Urtti, M. Yliperttula, Gold-embedded photosensitive liposomes for drug delivery: triggering mechanism and intracellular release, J. Controlled Release. 147 (2010) 136-143.

[16] N. Harris, M.J. Ford, M.B. Cortie, Optimization of plasmonic heating by gold nanospheres and nanoshells, The Journal of Physical Chemistry B. 110 (2006) 10701-10707.

[17] B. Bondurant, A. Mueller, D.F. O'Brien, Photoinitiated destabilization of sterically stabilized liposomes, Biochimica et Biophysica Acta (BBA)-Biomembranes. 1511 (2001) 113-122.

[18] T. Lajunen, L. Viitala, L. Kontturi, T. Laaksonen, H. Liang, E. Vuorimaa-Laukkanen, T. Viitala, X. Le Guével, M. Yliperttula, L. Murtomäki, Light induced cytosolic drug delivery from liposomes with gold nanoparticles, J. Controlled Release. 203 (2015) 85-98.

[19] L. Viitala, T. Lajunen, A. Urtti, T. Viitala, L. Murtomäki, Detection of Phase Transition in Photosensitive Liposomes by Advanced QCM, The Journal of Physical Chemistry C. 119 (2015) 21395-21403.

[20] A. Standard, Z136. 1. American national standard for the safe use of lasers. American National Standards Institute, Inc., New York. (1993).

[21] L. Viitala, S. Pajari, T. Lajunen, L. Kontturi, T. Laaksonen, P. Kuosmanen, T. Viitala, A. Urtti, L. Murtomäki, Photothermally Triggered Lipid Bilayer Phase Transition and Drug Release from Gold Nanorod and Indocyanine Green Encapsulated Liposomes, Langmuir. 32 (2016) 4554-4563.

[22] T. Lajunen, L. Kontturi, L. Viitala, M. Manna, O. Cramariuc, T. Róg, A. Bunker, T. Laaksonen, T. Viitala, L. Murtomäki, Indocyanine Green-Loaded Liposomes for Light-Triggered Drug Release, Molecular pharmaceutics. 13 (2016) 2095-2107.

[23] FDA, Product Insert: Indocyanine Green (IC-Green™), 2015 (2006).

[24] EMA, Evaluation of the pharmacokinetics of medicinal products in patients with impaired hepatic function, 2015 (2005).

[25] J.C. Kraft, R.J. Ho, Interactions of indocyanine green and lipid in enhancing near-infrared fluorescence properties: the basis for near-infrared imaging in vivo, Biochemistry (N. Y.). 53 (2014) 1275-1283.

[26] J. Hua, N. Gross, B. Schulze, U. Michaelis, H. Bohnenkamp, E. Guenzi, L.L. Hansen, G. Martin, H.T. Agostini, In vivo imaging of choroidal angiogenesis using fluorescence-labeled cationic liposomes, Mol. Vis. 18 (2012) 1045-1054.

[27] S.T. Proulx, P. Luciani, S. Derzsi, M. Rinderknecht, V. Mumprecht, J.C. Leroux, M. Detmar, Quantitative imaging of lymphatic function with liposomal indocyanine green, Cancer Res. 70 (2010) 7053-7062.

[28] T. Desmettre, J. Devoisselle, S. Mordon, Fluorescence properties and metabolic features of indocyanine green (ICG) as related to angiography, Surv. Ophthalmol. 45 (2000) 15-27.

[29] M.L. Landsman, G. Kwant, G.A. Mook, W.G. Zijlstra, Light-absorbing properties, stability, and spectral stabilization of indocyanine green, J. Appl. Physiol. 40 (1976) 575-583.

[30] W.R. Chen, R.L. Adams, K.E. Bartels, R.E. Nordquist, Chromophore-enhanced in vivo tumor cell destruction using an 808-nm diode laser, Cancer Lett. 94 (1995) 125-131.

[31] M. Sawa, K. Awazu, T. Takahashi, H. Sakaguchi, H. Horiike, M. Ohji, Y. Tano, Application of femtosecond ultrashort pulse laser to photodynamic therapy mediated by indocyanine green, Br. J. Ophthalmol. 88 (2004) 826-831.

[32] Y. Ma, S. Tong, G. Bao, C. Gao, Z. Dai, Indocyanine green loaded SPIO nanoparticles with phospholipid-PEG coating for dual-modal imaging and photothermal therapy, Biomaterials. 34 (2013) 7706-7714.

[33] A.L. Klibanov, K. Maruyama, V.P. Torchilin, L. Huang, Amphipathic polyethyleneglycols effectively prolong the circulation time of liposomes, FEBS Lett. 268 (1990) 235-237.

[34] X. Yan, G.L. Scherphof, J.A. Kamps, Liposome opsonization, J. Liposome Res. 15 (2005) 109-139.

[35] M. Çağdaş, A.D. Sezer, S. Bucak, Liposomes as potential drug carrier systems for drug delivery, in: Anonymous Application of Nanotechnology in Drug Delivery, InTech, 2014.

[36] V. Saxena, M. Sadoqi, J. Shao, Degradation kinetics of indocyanine green in aqueous solution, J. Pharm. Sci. 92 (2003) 2090-2097.

[37] A. Rimpelä, M. Schmitt, S. Latonen, M. Hagström, M. Antopolsky, J.A. Manzanares, H. Kidron, A. Urtti, Drug distribution to retinal pigment epithelium: studies on melanin binding, cellular kinetics, and single photon emission computed tomography/computed tomography imaging, Molecular pharmaceutics. 13 (2016) 2977-2986.

[38] S. Patel, G. Müller, J.O. Stracke, U. Altenburger, H. Mahler, D. Jere, Evaluation of protein drug stability with vitreous humor in a novel ex-vivo intraocular model, European Journal of Pharmaceutics and Biopharmaceutics. 95 (2015) 407-417.

[39] W.L. Jorgensen, D.S. Maxwell, J. Tirado-Rives, Development and testing of the OPLS all-atom force field on conformational energetics and properties of organic liquids, J. Am. Chem. Soc. 118 (1996) 11225-11236.

[40] W. Kulig, M. Pasenkiewicz-Gierula, T. Róg, Topologies, structures and parameter files for lipid simulations in GROMACS with the OPLS-aa force field: DPPC, POPC, DOPC, PEPC, and cholesterol, Data in brief. 5 (2015) 333-336.

[41] A. Maciejewski, M. Pasenkiewicz-Gierula, O. Cramariuc, I. Vattulainen, T. Rog, Refined OPLS all-atom force field for saturated phosphatidylcholine bilayers at full hydration, The Journal of Physical Chemistry B. 118 (2014) 4571-4581.

[42] W.L. Jorgensen, J. Chandrasekhar, J.D. Madura, R.W. Impey, M.L. Klein, Comparison of simple potential functions for simulating liquid water, J. Chem. Phys. 79 (1983) 926-935.

[43] M. Dzieciuch-Rojek, C. Poojari, J. Bednar, A. Bunker, B. Kozik, M. Nowakowska, I. Vattulainen, P. Wydro, M. Kepczynski, T. Róg, Effects of Membrane PEGylation on Entry and Location of Antifungal Drug Itraconazole and Their Pharmacological Implications, Molecular pharmaceutics. 14 (2017) 1057-1070.

[44] L.M. Crowe, J.H. Crowe, A. Rudolph, C. Womersley, L. Appel, Preservation of freeze-dried liposomes by trehalose, Arch. Biochem. Biophys. 242 (1985) 240-247.

[45] J.H. Crowe, A.E. Oliver, F.A. Hoekstra, L.M. Crowe, Stabilization of dry membranes by mixtures of hydroxyethyl starch and glucose: the role of vitrification, Cryobiology. 35 (1997) 20-30.

[46] J.A. Zhang, G. Anyarambhatla, L. Ma, S. Ugwu, T. Xuan, T. Sardone, I. Ahmad, Development and characterization of a novel Cremophor® EL free liposome-based paclitaxel (LEP-ETU) formulation, European journal of pharmaceutics and biopharmaceutics. 59 (2005) 177-187.

[47] O. Mertins, P.H. Schneider, A.R. Pohlmann, N.P. da Silveira, Interaction between phospholipids bilayer and chitosan in liposomes investigated by 31P NMR spectroscopy, Colloids and Surfaces B: Biointerfaces. 75 (2010) 294-299.

[48] K. Cieślik-Boczula, A. Koll, The effect of 3-pentadecylphenol on DPPC bilayers ATR-IR and 31P NMR studies, Biophys. Chem. 140 (2009) 51-56.

[49] E.J. Dufourc, C. Mayer, J. Stohrer, G. Althoff, G. Kothe, Dynamics of phosphate head groups in biomembranes. Comprehensive analysis using phosphorus-31 nuclear magnetic resonance lineshape and relaxation time measurements, Biophys. J. 61 (1992) 42-57.

[50] D.B. Fenske, Structural and motional properties of vesicles as revealed by nuclear magnetic resonance, Chem. Phys. Lipids. 64 (1993) 143-162.

[51] M. Stepniewski, M. Pasenkiewicz-Gierula, T. Róg, R. Danne, A. Orlowski, M. Karttunen, A. Urtti, M. Yliperttula, E. Vuorimaa, A. Bunker, Study of PEGylated lipid layers as a model for PEGylated liposome surfaces: molecular dynamics simulation and langmuir monolayer studies, Langmuir. 27 (2011) 7788-7798.

[52] A. Magarkar, T. Róg, A. Bunker, Molecular dynamics simulation of PEGylated membranes with cholesterol: building toward the DOXIL formulation, The Journal of Physical Chemistry C. 118 (2014) 15541-15549.

[53] A. Magarkar, T. Róg, A. Bunker, A computational study suggests that replacing PEG with PMOZ may increase exposure of hydrophobic targeting moiety, European Journal of Pharmaceutical Sciences. 103 (2017) 128-135.

[54] C. Chen, D. Han, C. Cai, X. Tang, An overview of liposome lyophilization and its future potential, J. Controlled Release. 142 (2010) 299-311.

[55] E.M. Del Amo, A. Rimpelä, E. Heikkinen, O.K. Kari, E. Ramsay, T. Lajunen, M. Schmitt, L. Pelkonen, M. Bhattacharya, D. Richardson, Pharmacokinetic aspects of retinal drug delivery, Prog. Retin. Eye Res. 57 (2017) 134-185.

[56] J. Senior, G. Gregoriadis, Stability of small unilamellar liposomes in serum and clearance from the circulation: the effect of the phospholipid and cholesterol components, Life Sci. 30 (1982) 2123-2136.

[57] M. Grit, D.J. Crommelin, Chemical stability of liposomes: implications for their physical stability, Chem. Phys. Lipids. 64 (1993) 3-18.

[58] D. Lasic, F. Martin, A. Gabizon, S. Huang, D. Papahadjopoulos, Sterically stabilized liposomes: a hypothesis on the molecular origin of the extended circulation times, Biochimica et Biophysica Acta (BBA)-Biomembranes. 1070 (1991) 187-192.

[59] F. Szoka Jr, D. Papahadjopoulos, Comparative properties and methods of preparation of lipid vesicles (liposomes), Annu. Rev. Biophys. Bioeng. 9 (1980) 467-508.

[60] A. Suganami, T. Toyota, S. Okazaki, K. Saito, K. Miyamoto, Y. Akutsu, H. Kawahira, A. Aoki, Y. Muraki, T. Madono, Preparation and characterization of phospholipid-conjugated indocyanine green as a near-infrared probe, Bioorg. Med. Chem. Lett. 22 (2012) 7481-7485.

[61] T. Toyota, H. Fujito, A. Suganami, T. Ouchi, A. Ooishi, A. Aoki, K. Onoue, Y. Muraki, T. Madono, M. Fujinami, Near-infrared-fluorescence imaging of lymph nodes by using liposomally formulated indocyanine green derivatives, Bioorg. Med. Chem. 22 (2014) 721-727.

[62] A. Suganami, Y. Iwadate, S. Shibata, M. Yamashita, T. Tanaka, N. Shinozaki, I. Aoki, N. Saeki, H. Shirasawa, Y. Okamoto, Liposomally formulated phospholipid-conjugated indocyanine green for intra-operative brain tumor detection and resection, Int. J. Pharm. 496 (2015) 401-406.

[63] J. Xing, D. Liu, G. Zhou, Y. Li, P. Wang, K. Hu, N. Gu, M. Ji, Liposomally formulated phospholipid-conjugated novel near-infrared fluorescence probe for particle size effect on cellular uptake and biodistribution in vivo, Colloids and Surfaces B: Biointerfaces. 161 (2018) 588-596.

[64] C. Leal, S. Rögnvaldsson, S. Fossheim, E.A. Nilssen, D. Topgaard, Dynamic and structural aspects of PEGylated liposomes monitored by NMR, J. Colloid Interface Sci. 325 (2008) 485-493.

[65] E. Burnell, P. Cullis, B. De Kruijff, Effects of tumbling and lateral diffusion on phosphatidylcholine model membrane 31P-NMR lineshapes, Biochimica et Biophysica Acta (BBA)-Biomembranes. 603 (1980) 63-69.

[66] R. Soong, P.M. Macdonald, PEG molecular weight and lateral diffusion of PEG-ylated lipids in magnetically aligned bicelles, Biochimica Et Biophysica Acta (BBA)-Biomembranes. 1768 (2007) 1805-1814.

[67] J.W. Holland, P.R. Cullis, T.D. Madden, Poly (ethylene glycol)− Lipid Conjugates Promote Bilayer Formation in Mixtures of Non-Bilayer-Forming Lipids, Biochemistry (N. Y.). 35 (1996) 2610-2617.

[68] K. Moribe, E. Tanaka, K. Maruyama, M. Iwatsuru, Enhanced encapsulation of amphotericin B into liposomes by complex formation with polyethylene glycol derivatives, Pharm. Res. 15 (1998) 1737-1742.

[69] K. Moribe, K. Maruyama, M. Iwatsuru, Encapsulation characteristics of nystatin in liposomes: effects of cholesterol and polyethylene glycol derivatives, Int. J. Pharm. 188 (1999) 193-202.

[70] N. Bertrand, P. Grenier, M. Mahmoudi, E.M. Lima, E.A. Appel, F. Dormont, J. Lim, R. Karnik, R. Langer, O.C. Farokhzad, Mechanistic understanding of in vivo protein corona formation on polymeric nanoparticles and impact on pharmacokinetics, Nature communications. 8 (2017) 777.

[71] C. Corbo, R. Molinaro, F. Taraballi, N.E. Toledano Furman, M.B. Sherman, A. Parodi, F. Salvatore, E. Tasciotti, Effects of the protein corona on liposome-liposome and liposome-cell interactions, Int. J. Nanomedicine. 11 (2016) 3049-3063.

[72] R.J. HAVEL, H.A. EDER, J.H. BRAGDON, The distribution and chemical composition of ultracentrifugally separated lipoproteins in human serum, J. Clin. Invest. 34 (1955) 1345-1353.

[73] P. Flodin, J. Killander, Fractionation of human-serum proteins by gel filtration, Biochim. Biophys. Acta. 63 (1962) 403-410.

[74] J. Figge, T.H. Rossing, V. Fencl, The role of serum proteins in acid-base equilibria, J. Lab. Clin. Med. 117 (1991) 453-467.

[75] D.J. Brown, P. Bishop, H. Hamdi, M.C. Kenney, Cleavage of structural components of mammalian vitreous by endogenous matrix metalloproteinase-2, Curr. Eye Res. 15 (1996) 439-445.

[76] B.A. Filas, Q. Zhang, R.J. Okamoto, Y. Shui, D.C. Beebe, Enzymatic Degradation Identifies Components Responsible for the Structural Properties of the Vitreous BodyStiffness and Adhesivity of the Vitreous, Invest. Ophthalmol. Vis. Sci. 55 (2014) 55-63.

[77] T. Hernández-Caselles, J. Villalaín, J.C. Gómez-Fernández, Influence of liposome charge and composition on their interaction with human blood serum proteins, Mol. Cell. Biochem. 120 (1993) 119-126.

[78] T. Allen, L. Cleland, Serum-induced leakage of liposome contents, Biochimica et Biophysica Acta (BBA)-Biomembranes. 597 (1980) 418-426.

[79] M.L. Immordino, F. Dosio, L. Cattel, Stealth liposomes: review of the basic science, rationale, and clinical applications, existing and potential, International journal of nanomedicine. 1 (2006) 297.

[80] V. Torchilin, Liposomes in drug delivery, in: Anonymous Fundamentals and Applications of Controlled Release Drug Delivery, Springer, 2012, pp. 289-328.

[81] L.S. Vermeer, B.L. De Groot, V. Réat, A. Milon, J. Czaplicki, Acyl chain order parameter profiles in phospholipid bilayers: computation from molecular dynamics simulations and comparison with 2 H NMR experiments, European Biophysics Journal. 36 (2007) 919-931.

[82] E.C. van Winden, W. Zhang, D.J. Crommelin, Effect of freezing rate on the stability of liposomes during freeze-drying and rehydration, Pharm. Res. 14 (1997) 1151-1160.

[83] B. Stark, G. Pabst, R. Prassl, Long-term stability of sterically stabilized liposomes by freezing and freeze-drying: Effects of cryoprotectants on structure, European Journal of Pharmaceutical Sciences. 41 (2010) 546-555.

[84] J. Li, M. Hu, H. Xu, X. Yu, F. Ye, K. Wang, X. Luan, L. Li, D. Zhang, Influence of type and proportion of lyoprotectants on lyophilized ginsenoside Rg3 liposomes, J. Pharm. Pharmacol. 68 (2016) 1-13.

Graphical abstract